Composite Structures 99 (2013) 69–75

Contents lists available at SciVerse ScienceDirect

Composite Structures

journal homepage: www.elsevier.com/locate/compstruct

Morphing wing flexible skins with curvilinear fiber composites

Senthil Murugan *, M.I. Friswell

College of Engineering, Swansea University, Singleton Park, Swansea SA2 8PP, UK

ARTICLE INFO

Article history:
Available online 17 December 2012

Keywords:
Morphing wing skins
Curvilinear fiber composites
Flexibility
Multi-objective optimization

ABSTRACT

Morphing aircraft wing skins require composites with conflicting structural requirements: low in-plane stiffness and high out-of-plane bending stiffness. In this study, composites with curvilinear fiber paths are examined to enhance these conflicting structural requirements. The numerical results show that curved fiber paths can minimize the in-plane stiffness and increase the bending stiffness simultaneously compared to a baseline plate with straight fibers. A flexibility ratio is defined to assess the in-plane and out-of-plane deformation of the plate, simultaneously. A multi-objective optimization is formulated to find optimal curved fiber paths which maximize the flexibility ratio of the morphing wing skin. The optimization is performed with fiber paths represented as independent discrete fibers and continuous curvilinear fibers. The results show a significant increase in the flexibility ratio compared to a baseline plate with straight fibers. The aspect ratio of plate, laminate stacking sequence and in-plane loading direction have considerable influence on the optimal paths of the curved fibers.

1. Introduction

Next generation aircraft require wings which can reconfigure to multiple shapes, each one of which is optimal at a specific flight condition. The aircraft wings capable of such a reconfiguration in flight are termed morphing wings [1,2]. One of the key challenges in developing a successful morphing wing is the development of a flexible skin which is a continuous layer of material that would stretch over a stiff morphing structure and forms a smooth aerodynamic surface [3,4]. These require composite skins with conflicting structural requirements: low in-plane stiffness and high out-of-plane bending stiffness. The low in-plane stiffness allows the skins to deform with less actuation force while high bending stiffness withstands the aerodynamic loads. Conventional composite laminates with straight fibers may not be the optimal choice as the in-plane stiffness of the laminate is high in the fiber direction and low in the orthogonal direction. This restricts the design space of fiber reinforced composites for morphing skin applications. However, the curvilinear fiber paths or spatial orientation of fiber angles introduce additional design variables that can be beneficial in achieving the in-plane and out-of-plane stiffness requirements.

Considerable research has focused on enhancing the static, dynamic and buckling behavior of composite structures with curved fiber (CVF) composites. A brief review of the studies focused on improving static performance of plates is discussed. Gurdal and Olmedo [5] studied the in-plane response of a symmetrically laminated composite panel with spatially varying fiber orientations. An iterative collocation technique was used to study the effects of spatial variation of fiber angle on the displacement fields, stress resultants, and global stiffness. Muc and Ulatowska [6] investigated the minimum compliance design of variable stiffness composite laminates by the Rayleigh–Ritz method. Local fiber orientation angles are treated as continuous design variables, and their spatial distribution is determined based on an optimality criterion formulation for minimum compliance design. The study showed a substantial gain in the bending stiffness by spatially orienting fiber angles in their optimal directions. Further, the results have shown that the optimal spatial distribution of fibers is strongly dependent on the plate geometry.

Setoodeh et al. [7] studied the optimal design of curved fiber composites for minimum in-plane and out-of plane compliance. The minimum compliance design problem was formulated in lamination parameters space and the lamination parameters were allowed to vary in a continuous manner over the domain. The results showed significant improvements in in-plane stiffness by spatially varying the fiber angles. In a similar study, a cellular automata (CA) methodology was used for the optimal design of curvilinear fiber paths to improve the in-plane response of composite laminae [8].

In addition to the above studies, the concurrent enhancement of multiple structural responses of composite plates such as in-plane compliance, strength and buckling load with CVF composites was also studied [9–11]. Gurdal et al. [9] studied the effects of fiber paths on the buckling load and the in-plane stiffness of composite plates. The results showed the existence of many fiber paths with equal buckling loads but with different global stiffness values, or

* Corresponding author. Tel.: +44 (0)1792 602969; fax: + 44 (0)1792 295676.
E-mail address: s.m.masanam@swansea.ac.uk (S. Murugan).

0263-8223/$ - see front matter © 2012 Elsevier Ltd. All rights reserved.
http://dx.doi.org/10.1016/j.compstruct.2012.11.026

vice versa. Alhajahmad et al. [10] studied the optimal fiber paths for maximum strength and buckling performance. The optimal results showed significant improvements in the strength and the buckling load of the structure compared to a quasi-isotropic design with straight fibers. The simultaneous optimization of maximum in-plane stiffness and buckling load of a composite laminate plate was studied in the multi-objective optimization framework with curvilinear fiber paths as design variables [11]. The results showed that curvilinear fiber paths can increase both buckling load and in-plane stiffness simultaneously compared to conventional straight fiber composites. Also, the optimum fiber paths depend on the loading direction and boundary conditions. The above studies clearly show the use of curvilinear fiber paths to enhance the multiple structural response of composite structures. However, no study has focused on the use of curvilinear fiber paths to minimize the in-plane stiffness and simultaneously maximize the out-of-plane bending stiffness of composite structures. Thus the objective of this study is to maximize the in-plane compliance while simultaneously minimizing the out-of-plane compliance to achieve the desired structural requirements of morphing skins.

In the first part of this study, the effects of spatial variation of fiber paths on the in-plane and out-of-plane response of composite plates with different aspect ratios are studied. The composite plates are modeled with the out-of-plane and in-plane boundary conditions representative of a morphing wing skin. An optimization problem is then formulated to minimize the in-plane stiffness while simultaneously maximizing the out-of-plane stiffness by considering the spatial variation of fiber angles as design variables. The fiber paths are represented with a discontinuous discrete representation and a continuous fiber representation. The optimization is performed for different aspect ratios with the genetic algorithm as the optimization tool.

2. Curvilinear fiber composites

In general, aircraft wing skins are made of balanced symmetric laminates to avoid undesired elastic couplings. For a balanced symmetric laminate of a variable stiffness composite, the constitutive equations in terms of force resultants (N_x, N_y, and N_{xy}) and moment resultants (M_x, M_y, and M_{xy}) can be given as

$$\begin{Bmatrix} N_x \\ N_y \\ N_{xy} \end{Bmatrix} = \begin{bmatrix} A_{11}(x,y) & A_{12}(x,y) & 0 \\ A_{11}(x,y) & A_{22}(x,y) & 0 \\ 0 & 0 & A_{66}(x,y) \end{bmatrix} \begin{Bmatrix} u_{o,x} \\ v_{o,y} \\ u_{o,y} + v_{o,x} \end{Bmatrix} \tag{1}$$

$$\begin{Bmatrix} M_x \\ M_y \\ M_{xy} \end{Bmatrix} = \begin{bmatrix} D_{11}(x,y) & D_{12}(x,y) & D_{16}(x,y) \\ D_{12}(x,y) & D_{22}(x,y) & D_{26}(x,y) \\ D_{16}(x,y) & D_{26}(x,y) & D_{66}(x,y) \end{bmatrix} \begin{Bmatrix} w_{o,xx} \\ w_{o,yy} \\ 2w_{o,xy} \end{Bmatrix} \tag{2}$$

where A_{ij} and D_{ij} are the elements of the in-plane and bending stiffness matrix of the composite plate, respectively [12]. The mid out-of-plane displacement is represented by w and in-plane displacements in the x and y directions are represented by u and v, respectively. The above equations show that the in-plane and out-of-plane displacements are independent and depend on A_{ij} and D_{ij}, respectively. The stiffness parameters are given by

$$A_{ij} = \sum_{k=1}^{n} Q_{ij}(z_k - z_{k-1}), \quad D_{ij} = \sum_{k=1}^{n} \frac{Q_{ij}}{3}(z_k^3 - z_{k-1}^3) \tag{3}$$

where the Q_{ij}s are the transformed reduced stiffness terms. The terms z_k and z_{k-1} are the upper and lower coordinates of the kth ply, respectively. The above relations show the in-plane stiffness of a CVF laminate is a function of the thickness of the plies $(z_k - z_{k-1})$ and spatial variation of the $Q_{ij}(x,y)$ which in turn is a function of the fiber angle. Similarly, the bending stiffness of the CVF laminate is a function of the spatial variation of fiber angle and the stacking sequence of plies, in addition to the thickness term $(z_k^3 - z_{k-1}^3)$.

3. Structural model of morphing skins

A morphing aircraft based on variable chord or variable camber concepts requires wing skins with low in-plane stiffness to allow a large in-plane deformation, and high out-of-plane bending stiffness to carry the aerodynamic loads. For example, a typical UAV wing or a helicopter rotor blade with variable chord extension is shown in Fig. 1. The wing skin extends from an initial position ABCD to ABEF. This portion of the wing skin can be modeled as a composite plate with boundary conditions representing those of the wing skin [4,13].

In this study, the composite plates are modeled for boundary conditions which allow the in-plane deformation while carrying the aerodynamic pressure loads. The boundary conditions for the out-of-plane deformation and in-plane behavior of the plate are shown in Fig. 2. The plate is simply supported at three sides and fixed at one side for the out-of-plane deformation and denoted as SSFF. Similarly, the plate is allowed to deform in the in-plane direction as shown in Fig. 2b. The ratio of length (L) to chord (B) of the plate is defined as the aspect ratio ($AR = L/B$). The length of plate represents the distance between the ribs of a wing where the plate is supported along the spanwise direction. The morphing wing skins are subjected to the aerodynamic loads and the in-plane actuation forces shown in Fig. 1 [13]. Generally, the aerodynamic pressure over the cross-section of a wing varies in the chord wise direction. However, the variation in aerodynamic pressure near the trailing edge portion is less than the variations near the leading edge of the wing. Therefore, a uniform pressure which represents the aerodynamic pressure is applied to the plate representing the skin [13,4]. Similarly, a uniform in-plane load to represent the actuation force is applied along the boundary CD of the plate as shown in Fig. 2b. The in-plane and out-of-plane deformations of the plate corresponding to these loads are simulated. The structural analysis is carried out with ANSYS using the SHELL281 elements. The modeling of laminated composite shells with SHELL281 is governed by the first order shear deformation theory [14].

From the morphing wing perspective, the change in in-plane area of the wing skin is a significant factor. The increase in the in-plane area (DCEF =δA) for a prescribed in-plane loading is calculated as shown in Fig. 2b. The morphing wing skins also require the minimum out-of-plane deformation to retain the aerodynamic performance of the wing [2,4]. Therefore, the maximum value of out-of-plane deformation (w_m) for the prescribed uniform pressure loading is calculated.

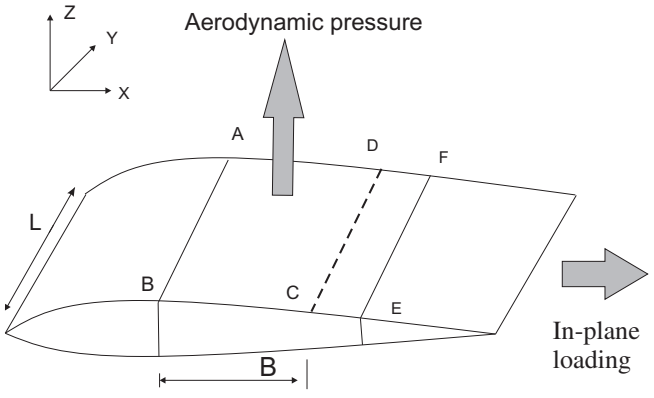

Fig. 1. Typical representation of morphing wing with chord extension.

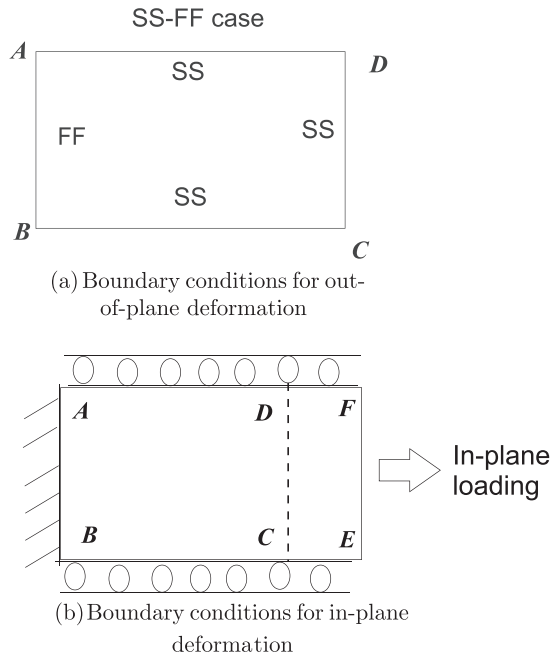

Fig. 2. Boundary conditions of morphing wing skins (SS-simply supported edge, FF-clamped edge).

The fiber paths of a variable stiffness composite plate can be defined in multiple ways. However, the fiber paths are limited by manufacturing constraints. Most of the studies on curved fiber composite define a linear, 1-D variation of a reference fiber path. This linear variation along the panel direction y can be given as

$$\theta(y) = 2(T_1 - T_o)\left|\frac{y}{B}\right| + T_o \tag{4}$$

where $\theta(y)$ represents the fiber orientation, B denotes the width of the plate, and T_1 and T_0 represent the fiber angles at the edge $(y = B/2)$ and middle of the plate $(y = 0)$, respectively. This reference fiber path, as shown in Fig. 3, can be repeated along the x direction to manufacture the CVF composite plate [9]. This fiber path definition of the single ply layer is generally represented as $\langle T_0|T_1\rangle$. The stacking sequence of a balanced symmetric CVF laminate with $2n$ plies can be given as $\left[\pm\langle T_o^k|T_1^k\rangle_n\right]_s$. The values of T_0 and T_1 are given in degrees in this study.

4. Numerical results

In the conventional wing design, the skin is generally made of straight fiber composites with $\pm 45^\circ$ plies. Therefore, the performance of the curved fiber composites are compared with a baseline composite plate with $\pm 45^\circ$ plies. Initially, the effects of the curved fiber paths on the in-plane δA and the maximum out-of-plane deformation (w_m) are studied for the aspect ratios 0.5, 1.0 and 2.0, as discussed in Section 3.

The plate is divided into $18 \times 36 = 648$ elements with 36 rows along the length L and 18 elements along each row as shown in Fig. 4. The number of elements is selected based on the convergence of in-plane and out-of-plane deformations. Also, in Ref. [15], the vibration of plates with curvilinear fibers is studied with the plate divided into $10 \times 10 = 100$ elements and plates with finer element divisions than the 100 element divisions showed similar numerical results.

Graphite/epoxy (CFRP) composite plies with elastic constants $E_y = 89.85$ GPa, $E_x = 5.81$ GPa, $G_{xy} = 2.04$ GPa, $\nu_{yx} = 0.32$ and thickness = 0.05 mm are used in this study. A uniform pressure of 50 Pa is applied to the surface and a uniform in-plane loading of 1 N/mm is applied along the edge of the plate. These out-of-plane and in-plane loads are selected from the morphing wing study given in Ref. [13]. A detailed discussion on the aeroelastic loading of wing is given in reference [13].

Initially, a parametric study is performed to study the in-plane and out-of-plane behavior of CVF composites. The parametric study is performed for three *AR*s of 0.5, 1.0 and 2.0. The chord of the plate (B) is considered to be constant with a value of 100 mm for all the *AR*s. A balanced symmetric laminate with four plies is considered for the parametric studies. The curvilinear fiber path is implemented in the FE model by dividing the plate into nine divisions along the chord and the elements in each division have the constant fiber angles obtained from Eq. (4).

To evaluate the potential benefits of CVF composites to the morphing skin application, the in-plane and out-of-plane deformations have to be calculated simultaneously. The ratio of change in the in-plane area (δA) to the maximum out-of-plane deflection (w_m) can be used to measure the performance of the CVF composites.

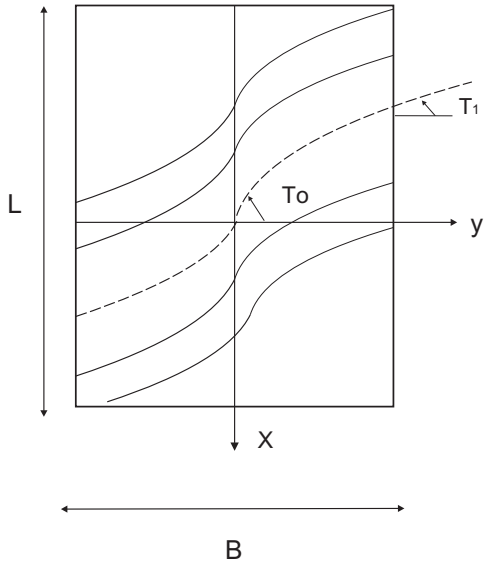

Fig. 3. Curved fiber paths in a composite plate.

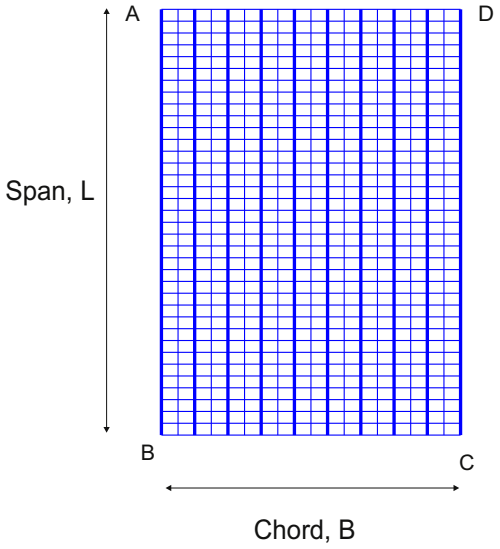

Fig. 4. FE model of the plate.

This ratio is defined as the flexibility ratio (FR $= \delta A/w_m$). The highest FR can be considered as optimal for the morphing skin requirements. The flexibility ratio is normalized with the values corresponding to the baseline plate with ±45°straight fibers (FR/FR^b) to measure the benefits of the CVF over straight fibers.

The variation of (FR/FR^b) with respect to the variation of $\langle T_o|T_1\rangle$ is evaluated for three *AR*s (0.5, 1.0 and 2.0). The variables T_0 and T_1 are varied from 0 to 90° and the corresponding structural deformations are measured for the specified in-plane and out-of-plane loadings. The numerical results are shown in Fig. 5. For *AR*s of 0.5 and 1.0, as shown in Fig. 5a and b, the non-dimenzionalised flexibility ratio (FR/FR^b) shows an increase of almost 700% and 150%, respectively. The maximum FR occurs for $\langle T_o|T_1\rangle$ equal to $\langle 90|90\rangle$. This corresponds to straight fibers which are perpendicular to the in-plane loading and the stiffness is dominated by E_x of the laminate, i.e., the matrix properties. However, there is also a considerable increase in the in-plane deformation for the fiber angles between $\langle 45|45\rangle$ and $\langle 90|90\rangle$. This region represents a composite with curved fiber paths for which T_0 is not equal to T_1. In contrast to *AR*s of 0.5 and 1.0, the FR is maximum when the fibers are curved (i.e., $T_o \neq T_1$) for *AR* of 2.0. The maximum FR is shown by arrows in Fig. 5c and the corresponding fiber paths are shown in Fig. 6. The FR show an increase up to 100%. These numerical results show the spatial representation of fiber paths have considerable influence on the FR and also vary with the *AR* of the laminate.

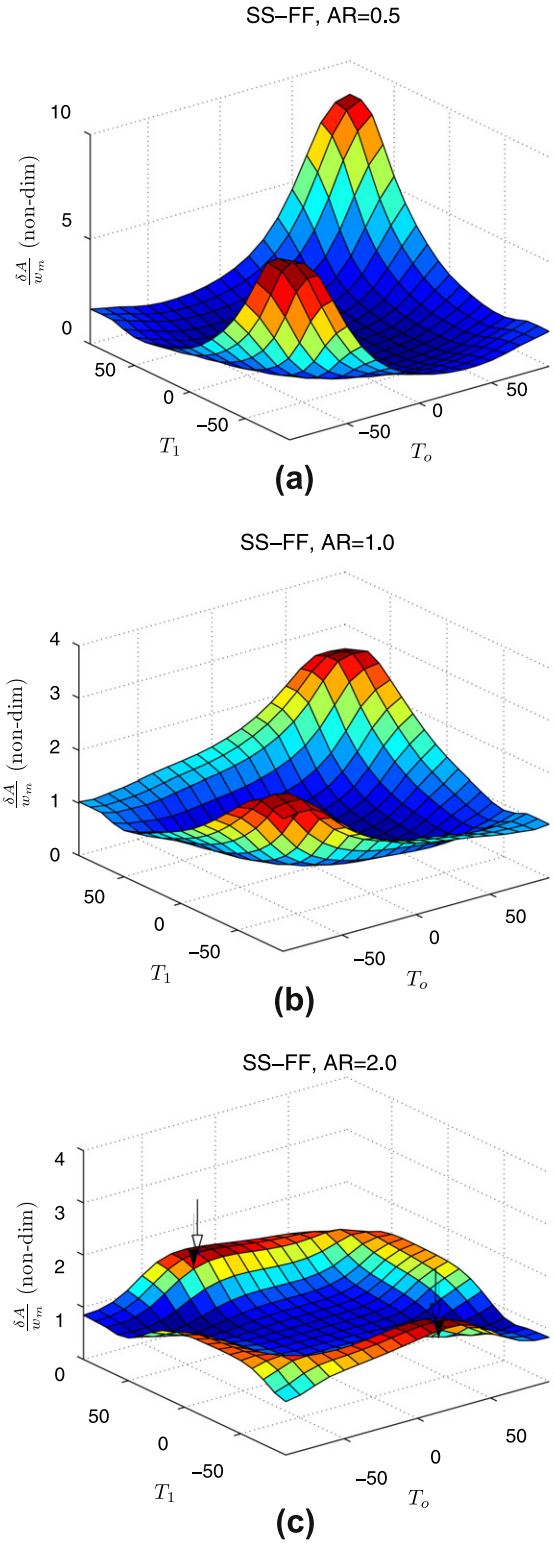

Fig. 5. Variation of flexibility ratio of the plate with curved fiber paths.

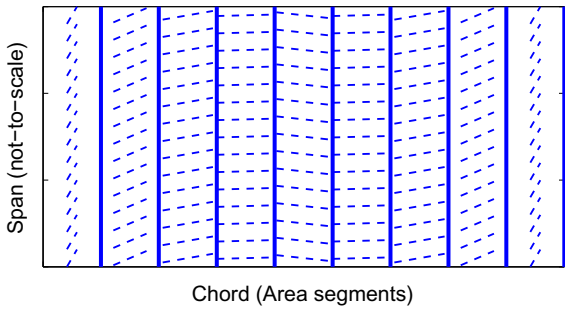

Fig. 6. Curved fiber paths of maximum FR, *AR* = 2.0.

5. Optimization problem

In the previous section, the parametric studies are performed with a balanced symmetric laminate with four plies given by $[\langle T_o|T_1\rangle/\langle -T_o|-T_1\rangle]_s$. The FR is plotted as a function of T_o and T_1 and the optimal fiber paths can be obtained from the plots. However, for a laminate with more than four plies or the fiber paths defined by functions other than the relation given in Eq. (4), an optimization formulation can be used to find the optimal fiber paths. Among numerous optimization methods, genetic algorithms (GAs) are most commonly used in the optimal design of constant stiffness and variable stiffness composite laminates [16,17]. GAs are preferred in the composite laminate optimization studies because of its simple coding, gradient free calculations and ease in handling the different types of objective functions and design variables [18].

The morphing skins require maximum in-plane deformation (δA) for the given actuation loadings and minimum out-of-plane deformation (w_m) in response to the aerodynamic loads. These two objectives are normalized with the corresponding values (δA^b and w_m^b) of the baseline plate with ±45° straight fibers and given as

$$\text{Minimize,} \quad J_1 = \left(\frac{\delta A(\theta_s)}{\delta A^b}\right)^{-1} \tag{5}$$

$$\text{Minimize,} \quad J_2 = \left(\frac{w_m(\theta_s)}{w_m^b}\right) \tag{6}$$

Here, the design variable θ_s represent the spatial variation of fiber angles.

The optimization is performed for two cases with fibers represented as discrete fibers and continuous fibers. The optimization with discrete fiber representation is performed to explore the

spatial anisotropy of variable stiffness composites [17]. Therefore, the optimization is carried out for *AR*s of 0.5, 1.0 and 2.0. The optimization is performed as a single objective function with a weighted sum approach used to combine the two objective functions.

In the second case with continuous fiber path representation, the optimization is performed with specific consideration of the morphing skin application. The optimization is performed for an *AR* of 2.0 which is more representative of morphing skin applications. Further, the optimization in this case is performed with multi-objective genetic algorithm based on the non-dominated sorting genetic algorithm (NSGA-II) [19,17].

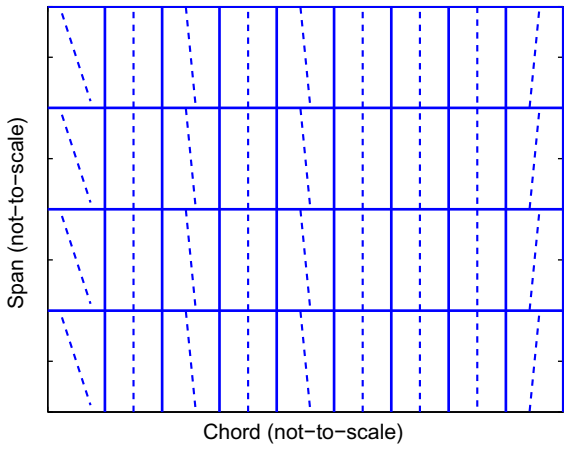

(a) 9 design variables, AR 0.5

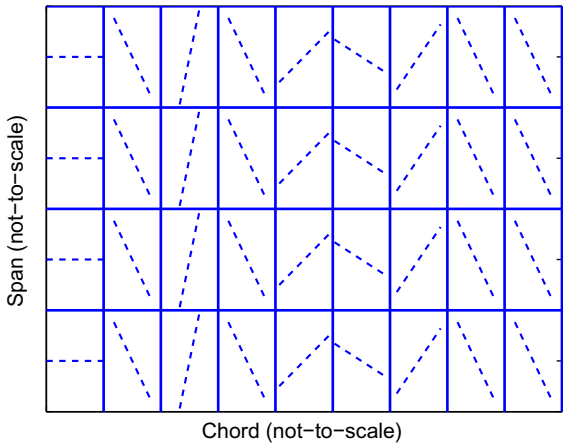

(b) 9 design variables, AR 1.0

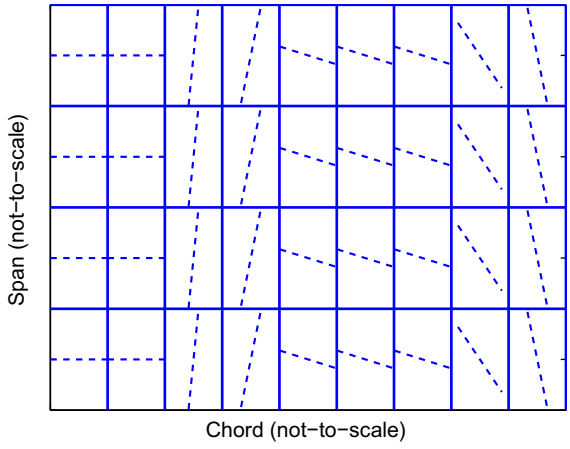

(c) 9 design variables, AR 2.0

Fig. 7. Optimal distribution of discrete fibers.

5.1. Discrete fiber

In this case, the plate is divided along the chord *B* into nine divisions with each division parallel to the span *L* [2]. The fiber orientation of each division is considered as design variable with a total of nine design variables. A weighted sum approach is used to combine the two objective functions and given as

$$\text{Minimize}, \quad J = a_1 J_1(X) + a_2 J_2(X) \tag{7}$$

$$X = [\theta_n], \quad n = 1, 9 \tag{8}$$

where a_1 and a_2 are the weights of the functions. Equal weights are assigned to both of the objective functions, i.e., $a_1 = 0.5$ and $a_2 = 0.5$. As this discrete fiber case is used to demonstrate the advantage of spatial discretization, only single objective optimization is performed. However, a Pareto optimization is performed in the continous fiber case. The optimization is performed with the GA coupled to the FE analysis in ANSYS. The optimal solutions are shown in Fig. 7, respectively. For an *AR* of 0.5, the FR is 700% higher

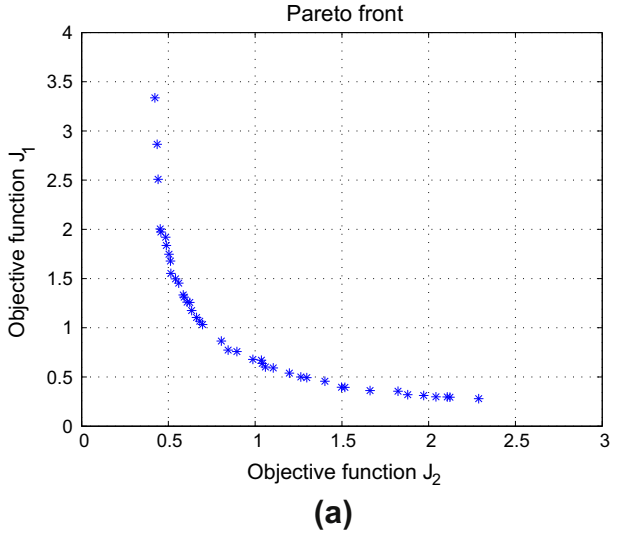

(a)

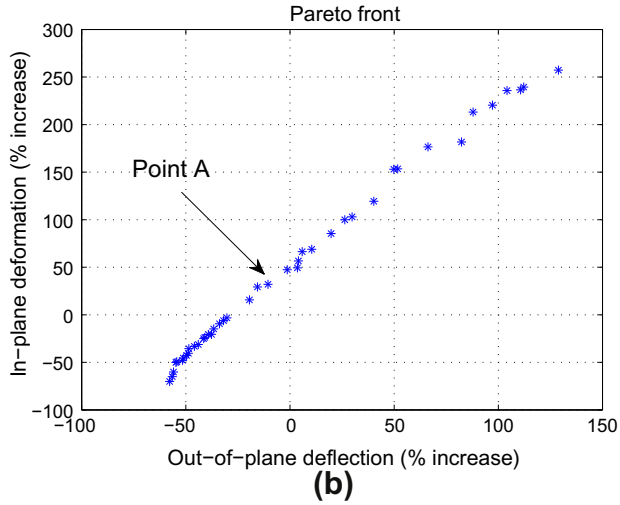

(b)

Fig. 8. Pareto-optimal solutions.

Table 1
Pareto-optimal solutions.

No.	In-plane deformation (% increase)	Out-of-plane deformation (% reduction)	Curved fiber angles $[\pm\langle T_o^k \vert T_1^k\rangle_4]$
1	47	2	$[\pm\langle 49\vert 27\rangle, \pm\langle 65\vert 33\rangle, \pm\langle 75\vert 64\rangle, \pm\langle 70\vert 68\rangle]$
2	32	11	$[\pm\langle 20\vert 40\rangle, \pm\langle 45\vert 63\rangle, \pm\langle 63\vert 75\rangle, \pm\langle 51\vert 66\rangle]$
3	30	16	$[\pm\langle 14\vert 41\rangle, \pm\langle 32\vert 70\rangle, \pm\langle 65\vert 65\rangle, \pm\langle 61\vert 77\rangle]$
4	16	20	$[\pm\langle 28\vert 20\rangle, \pm\langle 82\vert 46\rangle, \pm\langle 63\vert 71\rangle, \pm\langle 73\vert 70\rangle]$

than its baseline value. The optimal results show fiber paths almost perpendicular to the in-plane loading direction. For the *ARs* of 1.0 and 2.0, the FR shows an increase of 80 and 150 percent, respectively. The corresponding optimal results show fiber paths which are curved along the edge CD of the plate.

5.2. Continuous fiber path

In this case, a balanced symmetric laminate with 16 plies is considered and the total thickness is considered to be equal to the thickness of the laminates with 4 plies in the previous cases. The continuity of fibers is maintained by representing the fiber paths with Eq. (4). The curved fiber laminate with 16 plies can be represented as $\left[\pm\langle T_o^k \vert T_1^k\rangle_4\right]_s$ where T_o^k and T_1^k represent the design variables of the kth ply. This formulation gives 8 design variables. The in-plane and out-of-plane loading conditions are identical to those in the previous section.

$$\text{Minimize,} \quad J = [J_1(X), J_2(X)] \tag{9}$$

$$\text{where} \quad X = \left[\left\langle T_o^1 \vert T_1^1\right\rangle, \left\langle T_o^2 \vert T_1^2\right\rangle, \left\langle T_o^3 \vert T_1^3\right\rangle, \left\langle T_o^4 \vert T_1^4\right\rangle\right]$$

The multi-objective genetic algorithm based on the non-dominated sorting genetic algorithm (NSGA-II) is used to obtain the Pareto-optimal solutions [19]. The multi-objective optimization is performed with MATLAB with a population of 120, Pareto fraction value of 0.35 and the number of generations as 1000 [20].

The Pareto-optimal solutions are shown in Fig. 8. The Pareto front in Fig. 8a shows four optimal solutions for which the values of both the objective functions J_1 and J_2 are less than 1. For easy of understanding, the Pareto-front is replotted in terms of the in-plane and out-of-plane deformation as shown in Fig. 8b. The optimal solutions shows an almost linear increase in the out-of-plane deformation while the in-plane deformation is maximized. However, the optimal solutions near the optimal point A, as shown in Fig. 8b, show an increase of 30–50% in the in-plane flexibility while the out-of-plane deformations are reduced by 2–10%. This show the curved fibers can be used to increase the in-plane flexibility while simultaneously minimizing the out-of-plane deformation.

The Pareto-optimal solutions for which the in-plane deformation is increased while the out-of-plane deformation is reduced are given in Table 1. The curved fibers corresponding to optimal point 1 in Table 1 is shown in Fig. 9. From the optimal T_0 and T_1 values given in Table 1, the plies (plies 1 and 2) which are away from the neutral axis of the laminate tends to be curved along the chord of the plate while the plies closer to the neutral axis (plies 3 and 4) tends to be curved along the span of the plate. The results of parametric and optimization studies show the use of CVF composites for small scale morphing wings can be highly beneficial compared to straight fiber composites.

In this study, the optimization is performed as an unconstrained optimization problem. However, the manufacturing constraints have to be added to realize the laminates with curved fibers. Advanced manufacturing techniques such automated fiber placement techniques are currently used to realize the curved fiber composites. This techniques require the maximum allowable curvature of fiber path to be less than 3.28 m^{-1}. A detailed discussion on the manufacturing techniques and constraints can be inferred from references [21,22,17].

6. Conclusion

In this study, the effect of curved fiber paths on the in-plane flexibility and out-of-plane bending stiffness of composite plates representative of a morphing wing skin is studied. Initially, the effects of fiber paths on the in-plane and out-of-plane deformation is studied for various boundary conditions and aspect ratios. A flexibility ratio is defined to assess both the in-plane and out-of-plane deformation simultaneously. A multi-objective optimization problem is then formulated to maximize the flexibility ratio of the plate. The optimization is performed with curvilinear fiber paths represented as independent discrete fibers and also continuous fiber representations. The following conclusions are drawn from this study:

1. The parametric study is performed with curvilinear fibers represented as a function of two variables, T_0 and T_1. The flexibility ratio shows an increase of 700% and 150% for the plate with *AR*s of 0.5 and 1.0, respectively. The FR is maximum when the fibers are straight and perpendicular to the direction of in-plane loading. However, there is also a significant increase in the FR when

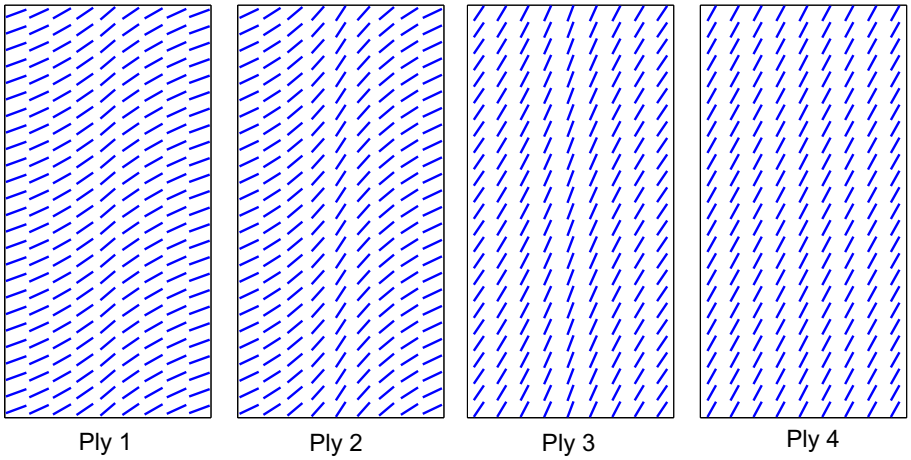

Fig. 9. Optimal curvilinear fiber paths.

the fibers are curved. For the plate with *AR* of 2.0, the FR shows an increase of 100%. The maximum FR occurs when the fibers are curved. These results show the curved fiber paths have considerable influence on the in-plane flexibility and out-of-plane bending behavior of the plate and also vary with the *AR* of the plate.

2. An optimization is performed with the spatial variation of fibers represented as discrete fibers. The optimal results show an increase of 700% in the FR for the plate with an *AR* of 0.5. The optimal solutions are almost straight fibers that are perpendicular to the in-plane loading direction. For the plate with *AR*s of 1.0 and 2.0, the optimal results show an increase of 80% and 150%, respectively. The optimal fiber paths are curved along the in-plane loading direction.
3. A multi-objective optimization is performed with the spatial variation of fibers represented as continuous curvilinear fibers. The Pareto-optimal solutions are obtained by using the non-dominated sorting genetic algorithm. The Pareto-optimal solutions show an increase of 15–50% in the in-plane flexibility while the out-of-plane deformations are reduced by 2–20%, simultaneously. The plies which are away from the neutral axis of the laminate tend to be curved while the plies near to the neutral axis tend to be straight fibers. The numerical results show the curvilinear fibers can be beneficial to meet the conflicting design requirements of morphing wing skins.

Acknowledgement

The authors acknowledge the support of the European Research Council through Project 247045 entitled "Optimization of Multi-scale Structures with Applications to Morphing Aircraft.

References

[1] Sofla AYN, Meguid SA, Tan KT, Yeo WK. Shape morphing of aircraft wing: status and challenges. Mater Des 2010;31(3):1284–92. http://dx.doi.org/10.1016/j.matdes.2009.09.011.
[2] Barbarino S, Bilgen O, Ajaj RM, Friswell MI, Inman DJ. A review of morphing aircraft. J Intell Mater Syst Struct 2011;22(9):823–77. http://dx.doi.org/10.1177/1045389X11414084.
[3] Thill C, Etches J, Bond I, Potter K, Weaver P. Morphing skins. Aeronaut J 2008;112(1129):117–39.
[4] Murugan S, Saavedra Flores EI, Adhikari S, Friswell MI. Optimal design of variable fiber spacing composites for morphing aircraft skins. Compos Struct 2012;94(5):1626–33. http://dx.doi.org/10.1016/j.compstruct.2011.12.023.
[5] Gurdal Z, Olmedo R. In-plane response of laminates with spatially varying fibre orientations: variable stiffness concept. AIAA J 1993;31(4):751–8.
[6] Muc A, Ulatowska A. Design of plates with curved fibre format. Compos Struct 2010;92(7):1728–33. http://dx.doi.org/10.1016/j.compstruct.2009.12.015.
[7] Setoodeh S, Abdalla MM, Gurdal Z. Design of variable stiffness laminates using lamination parameters. Compos Part B: Eng 2006;37(4–5):301–9. http://dx.doi.org/10.1016/j.compositesb.2005.12.001.
[8] Setoodeh S, Gurdal Z, Watson LT. Design of variable-stiffness composite layers using cellular automata. Comput Methods Appl Mech Eng 2006;195(9–12):836–51. http://dx.doi.org/10.1016/j.cma.2005.03.005.
[9] Gurdal Z, Tatting B, Wu C. Variable stiffness composite panels: effects of stiffness variation on the in-plane and buckling response. Compos Part A: Appl Sci Manuf 2008;39(5):911–22. http://dx.doi.org/10.1016/j.compositesa.2007.11.015.
[10] Alhajahmad A, Abdalla MM, Gurdal Z. Optimal design of tow-placed fuselage panels for maximum strength with buckling considerations. J Aircraft 2010;47(3):775–82. http://dx.doi.org/10.2514/1.40357.
[11] Nik MA, Fayazbakhsh K, Pasini D, Lessard L. Surrogate-based multi-objective optimization of a composite laminate with curvilinear fibers. Compos Struct 2012;94(8):2306–13. http://dx.doi.org/10.1016/j.compstruct.2012.03.021.
[12] Kasapoglou C. Design and analysis of composite structures: with applications to aerospace structures. Wiley; 2010.
[13] Barbarino S, Gandhi F, Webster S. Design of extendable chord sections for morphing helicopter rotor blades. J Intell Mater Syst Struct 2011;22(9):891–905.
[14] ANSYS. Release 11.0 Documentation for ANSYS. ANSYS, Inc.; 2007.
[15] Honda S, Narita Y. Vibration design of laminated fibrous composite plates with local anisotropy induced by short fibers and curvilinear fibers. Compos Struct 2011;93(2):902–10. http://dx.doi.org/10.1016/j.compstruct.2010.07.003.
[16] Ghiasi H, Fayazbakhsh K, Pasini D, Lessard L. Optimum stacking sequence design of composite materials Part II: Variable stiffness design. Compos Struct 2010;93(1):1–13. http://dx.doi.org/10.1016/j.compstruct.2010.06.001.
[17] Honda S, Igarashi T, Narita Y. Multi-objective optimization of curvilinear fiber shapes for laminated composite plates by using nsga-ii. Compos Part B: Eng 2012. http://dx.doi.org/10.1016/j.compositesb.2012.07.056. <http://www.sciencedirect.com/science/article/pii/S1359836812005173>.
[18] Ghiasi H, Pasini D, Lessard L. Optimum stacking sequence design of composite materials Part I: Constant stiffness design. Compos Struct 2009;90(1):1–11.
[19] Deb K. Multi-objective optimization using evolutionary algorithms, Wiley-Interscience series in systems and optimization. Chichester: John Wiley & Sons; 2001.
[20] MATLAB, version 7.10.0. The MathWorks Inc., Natick, Massachusetts; 2010.
[21] Akhavan H, Ribeiro P. Natural modes of vibration of variable stiffness composite laminates with curvilinear fibers. Compos Struct 2011;93(11):3040–7. http://dx.doi.org/10.1016/j.compstruct.2011.04.027. <http://www.sciencedirect.com/science/article/pii/S0263822311001516>.
[22] Kim BC, Potter K, Weaver PM. Continuous tow shearing for manufacturing variable angle tow composites. Compos Part A: Appl Sci Manuf 2012;43(8):1347–56. http://dx.doi.org/10.1016/j.compositesa.2012.02.024. <http://www.sciencedirect.com/science/article/pii/S1359835X12000929>.